



# Dynamic change of land use/land cover patterns and driving factors of Nansihu Lake Basin in Shandong Province, China

Fang Wang<sup>1,2,3</sup> · Xingzhong Yuan<sup>1,2</sup> · Xiaoping Xie<sup>4</sup>

Received: 2 January 2020 / Accepted: 4 February 2021 / Published online: 25 February 2021  
© The Author(s), under exclusive licence to Springer-Verlag GmbH, DE part of Springer Nature 2021

## Abstract

Anthropogenic activities and natural factors have a significant effect on land use/land cover (LULC) patterns of Nansihu Lake basin. Understanding the LULC change is essential for regional sustainable development. Based on LULC change detection methods, we characterized the spatial-temporal change of LULC patterns. Logistic regression model and the Conversion of Land Use and its Effects at Small regional extent (CLUE-S) model were used in driving factors analysis and scenario simulation. The results showed that cultivated land and construction land were the dominant LULC types. As construction land gradually expanded to the surrounding areas, a large amount of cultivated land was occupied, especially in the peripheral areas of the central cities. During 1987–2017, 4109.22 km<sup>2</sup> of cultivated land was converted into construction land, accounting for 86.38% of cultivated land change, and the contribution rate to construction land was 95.24%. Because of the severe drought in 2002, waters first decreased and then increased. The dynamic degree of waters reached 2.11%, and the increment of waters was mainly converted from cultivated land and unused land. The degree of LULC fragmentation was strengthened, and the distribution showed a diversified trend. The LULC changes were deeply influenced by natural environment and socio-economic factors. Under different scenarios, the expansion of construction land and occupation of cultivated land will continue to be the main features of LULC changes in the future. The LULC patterns will become more regular and more aggregated. This study can help address the interwoven challenges of urbanization development and ecological protection.

**Keywords** Land use/land cover patterns · Dynamic change · Driving factors · Scenario simulation · Nansihu Lake basin of Shandong Province

## Introduction

- ✉ Xingzhong Yuan  
1072000659@qq.com
- ✉ Xiaoping Xie  
xp.xie@263.net
- Fang Wang  
wangfang5445@163.com

<sup>1</sup> State Key Laboratory of Coal Mine Disaster Dynamics and Control, Chongqing University, Chongqing 400030, China

<sup>2</sup> Faculty of Architecture and Urban Planning, Chongqing University, Chongqing 400030, China

<sup>3</sup> Key Laboratory of the Three Gorges Reservoir Region's Eco-Environment, Ministry of Education, Chongqing University, Chongqing 400044, China

<sup>4</sup> College of Geography and Tourism, Key Laboratory of Nansihu Lake Wetland Ecological and Environmental Protection in Shandong Province, Qufu Normal University, Rizhao 276826, China

Land use is one of the key forms of human impacts on the natural environment, thereby resulting in changes of land cover which provide fundamental information related to the biophysical properties of the earth's land surfaces (Batunacun et al. 2018; Minta et al. 2018). The land use/land cover (LULC) pattern is a spatial arrangement and combination of various LULC types and represents the spatial expressional forms of heterogeneity (Duarte et al. 2018). Change in LULC patterns has accelerated during recent decades mostly because of anthropogenic factors and other natural events (Bertolo et al. 2012; Joorabian Shooshtari et al. 2020). Understanding the patterns, regional differences, driving factors and scenario simulation of LULC changes are fundamental for assessing LULC dynamics and essential for sustainable development (Joorabian Shooshtari et al. 2020; Shooshtari and Gholamalifard 2015).

Many LULC pattern metrics have been developed to reflect the LULC structural composition and spatial configuration characteristics (Alhamad et al. 2011; Hou et al. 2020; Statuto et al. 2019). LULC pattern indices have been proven as the important indicators for dominance, aggregation, connectivity, fragmentation, heterogeneity and diversity (Achmad et al. 2015; De Clercq et al. 2006; Malandra et al. 2019; Plexida et al. 2014). LULC patterns change has a profound effect on ecosystem structure and function (Malandra et al. 2019). More and more studies have explored the relationship between LULC patterns and driving factors (Feng et al. 2018; Li et al. 2017; Wan et al. 2015). Logistic regression can effectively analyse the relationships between multiple independent variables and a binary dependent variable (Mengistie et al. 2015; Olena et al. 2013; Peng et al. 2017). Further scenario simulation analysis based on a LULC change history and statistical relations between LULC and driving factors can provide more scientific and well-defined criteria in evaluating alternative land management and environmental protection strategies. The Conversion of Land Use and its Effects at Small regional extent (CLUE-S) model has been recognized as an efficient method, as proved by certain case studies (Overmars et al. 2007; Verburg et al. 2002; Waiyusri et al. 2016). The LULC demand, which is an essential non-spatial module of the CLUE-S model, needs to be predicted by other models, and Markov models have been widely applied to temporal LULC change prediction (Hu et al. 2013). The composite model consisted of the CLUE-S and Markov models can overcome their respective deficiencies in LULC demand prediction and spatial allocation, and thus can effectively improve the accuracy of LULC simulation.

The Nansihu Lake basin of Shandong Province is a crucial production base of grain, fisheries, coal and energy in both Shandong Province and China as a whole. Some mining activities in the basin started in the 1980s and continue today (Sun et al. 2019). Over the past 30 years, the mining subsidence had a certain extent effect on LULC patterns. Since the twenty-first century, the economy has increased rapidly with the growth rate is about to 8.61%. The urban population has more than doubled between 2000 and 2017, surging from 21 to 49%. The LULC patterns had undergone some significant changes. Therefore, further understanding the LULC patterns change in Nansihu Lake basin of Shandong Province is of great importance for understanding the ecological status and sustainable development. Despite the numerous studies concerning LULC patterns have been carried out at the basin scale (Mehrian et al. 2016; Schneider and Pontius 2001; Shooshtari and Gholamalifard 2015), a joint analysis of LULC patterns change, driving factors and scenario simulation has not been conducted as frequently.

The scale effect of LULC patterns is a prerequisite for accurately understanding its characteristic (Wu 2004).

However, LULC change detection methods rarely used at grid scale. We introduce the LULC gradient method, which is based on a grid, can effectively compare the regional differences in LULC patterns change. Therefore, by combining the LULC pattern index, dynamic change index, LULC transfer matrix and LULC gradient, this paper aims to reveal the dynamic change of LULC patterns in Shandong Nansihu Lake basin from 1987 to 2017. The driving factors of LULC patterns were analysed using a logistic regression model. Based on CLUE-S model, the differences in LULC patterns evolution under different simulated scenarios from 2017 to 2047 were further analysed. This study can provide theory support for land management decision-making and urban planning. It can also provide a reference to resolve the contradiction between economic development and land-use balance.

## Materials and methods

### Study area

The Nansihu Lake basin of Shandong Province contains 28 counties and districts of Jining, Zaozhuang, Heze and Tai'an Cities (Fig. 1), which lies between 34°27'4"N and 35°58'55"N and between 114°49'1"E and 117°49'48"E, covering an area of approximately 29,000 km<sup>2</sup>. Nansihu Lake is the largest freshwater lake in northern China and is one of the main hydro-junctions for water regulation and transfer in the eastern route of the South-to-North Water Transfer Project (Zhang et al. 2016). It comprises four lakes from north to south, namely, Nanyang, Dushan, Zhaoyang and Weishan. The eastern part of the study area is composed of low hilly areas and piedmont alluvial plain, and the western part is the Yellow River floodplain. It is obviously higher in the east than in the west (Li et al. 2013).

### Data source and processing

Landsat Thematic Mapper (TM) and Operational Land Imager (OLI) images of 1987, 2002 and 2017 were obtained from the Geo-spatial Data Cloud Platform (<http://www.gscloud.cn/>). All the images were acquired from April to September during the vigorous growing season of vegetation, with low cloud cover (Table 1). The remote sensing images were processed by radiance calibration and atmospheric correction to eliminate atmospheric effects. The Classification and Regression Tree (CART) decision tree classification method was used to interpret the LULC data of Shandong Nansihu Lake basin (Fig. 2). The CART algorithm was a non-parametric and rule-based machine learning method that attempted to inductively discover the set of rules from class-specific training samples which were acquired by the

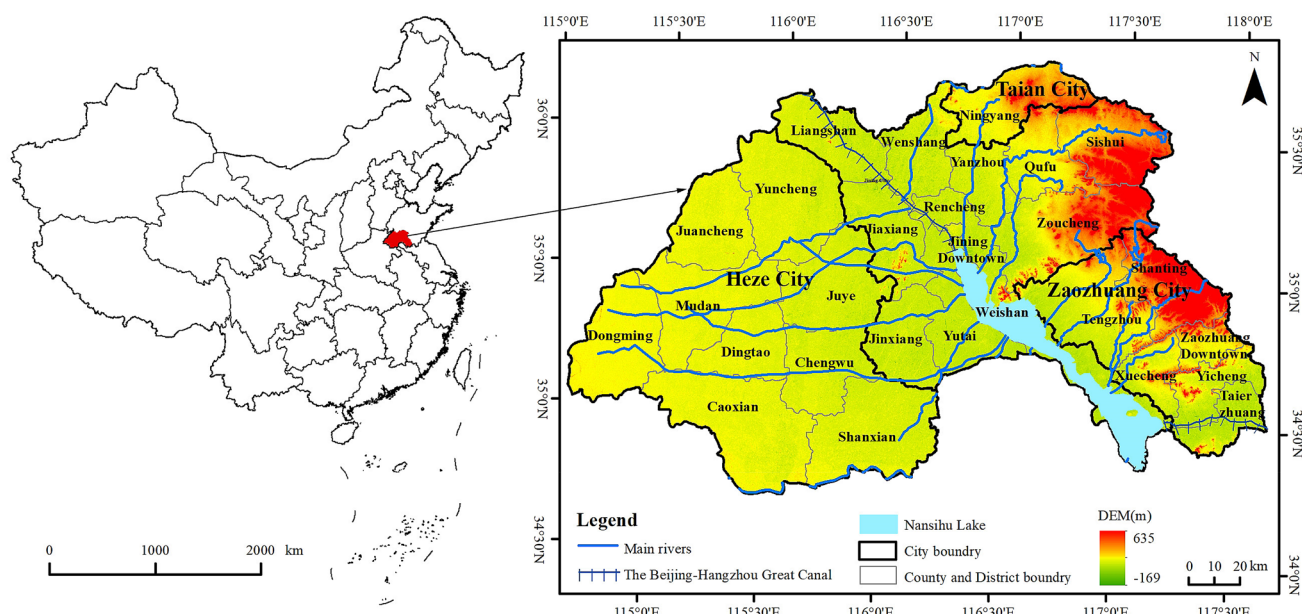


**Fig. 1** Location of the study area

**Table 1** Main attributes of Landsat images used in this study

Year	Satellite/Sensor	Acquisition date/Cloud cover (%)				
		121/36	122/35	122/36	123/35	123/36
1987	Landsat 5/TM	1987-08-11/6.98	1987-09-19/0	1987-09-19/0	1987-09-10/0	1987-08-25/0
2002	Landsat 5/TM	2002-04-14/0	2002-07-10/0	2002-07-10/0.01	2002-06-15/1.24	2002-04-12/0.03
2017	Landsat 8/OLI	2017-04-23/0.09	2017-04-30/1.18	2017-04-30/0.06	2017-07-10/0.2	2017-05-07/1.52

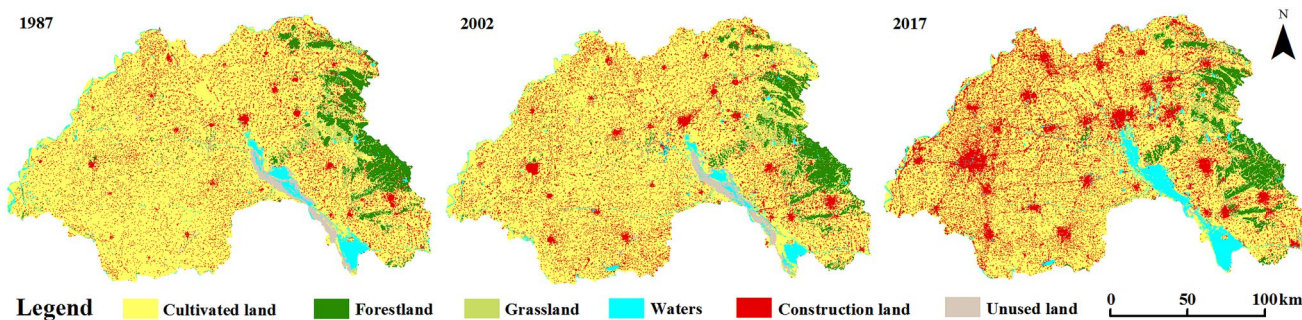


**Fig. 2** LULC type maps of Shandong Nansihu Lake basin

Region of Interest selection tool in the multivariate datasets. The multivariate datasets were composed of the original multi-spectral TM/OLI images, normalized difference vegetation index (NDVI), ISODATA unsupervised classification map and digital elevation model (DEM) data. The rules were represented in a structure referred to as a decision tree, which can generate automatically with the extension tool RuleGen of ENVI5.3. Each image was then classified according to the decision tree rules, and the LULC raster

data with a resolution of 30 m was finally produced after image classification post-processing, union, clip and format conversion analysis. The accuracy was assessed using a confusion matrix based on the sample points from Google Earth, with an overall classification accuracy greater than 80%. According to the second national land survey procedures (TD/T1014-2007), the LULC was divided into six first-level types, including cultivated land, forestland, grassland, waters, construction land and unused land.

Based on the principles of scientific validity, representativeness and accessibility, twelve natural environment and socio-economic factors were selected to build the logistic driving factors database (Liu et al. 2017). This research employed the ASTER GDEM V2 Digital elevation model data from the Geo-spatial Data Cloud Platform for altitude and slope extraction. The gross domestic product (GDP), population (POP), temperature and precipitation data were derived from the Resource and Environmental Science Data Center (<http://www.resdc.cn/>) of the Chinese Academy of Sciences. The distance variables related to cities, railways, highways, county roads, rivers and coal mine areas were calculated from the basic geographical information data of China.

## Methods

The structure framework of the methodology used in this research is summarized in Fig. 3.

### LULC change detection methods

On the basis of previous studies (Abdolalizadeh et al. 2019; Jenerette and Wu 2001; Zhang et al. 2019), LULC pattern indices were calculated using the Fragstats 4.2 software in the present study.

With reference to the related studies (Cui and Wang 2015; Wang et al. 2017; Yu et al. 2010), two dynamic change indices, named the single and comprehensive LULC dynamic degrees, were applied to understand the evolution characteristics of LULC structure and ratio. The equations are as follows:

$$K = \frac{U_b - U_a}{U_a} \times \frac{1}{T} \times 100\% \quad (1)$$

where  $K$  denotes the dynamic degree,  $U_a$  and  $U_b$  denote the area of LULC type in the beginning and at the end of the study period, respectively.

$$LC = \frac{\sum_{i=1}^n \Delta LU_{i-j}}{2LU} \times \frac{1}{T} \times 100\% \quad (2)$$

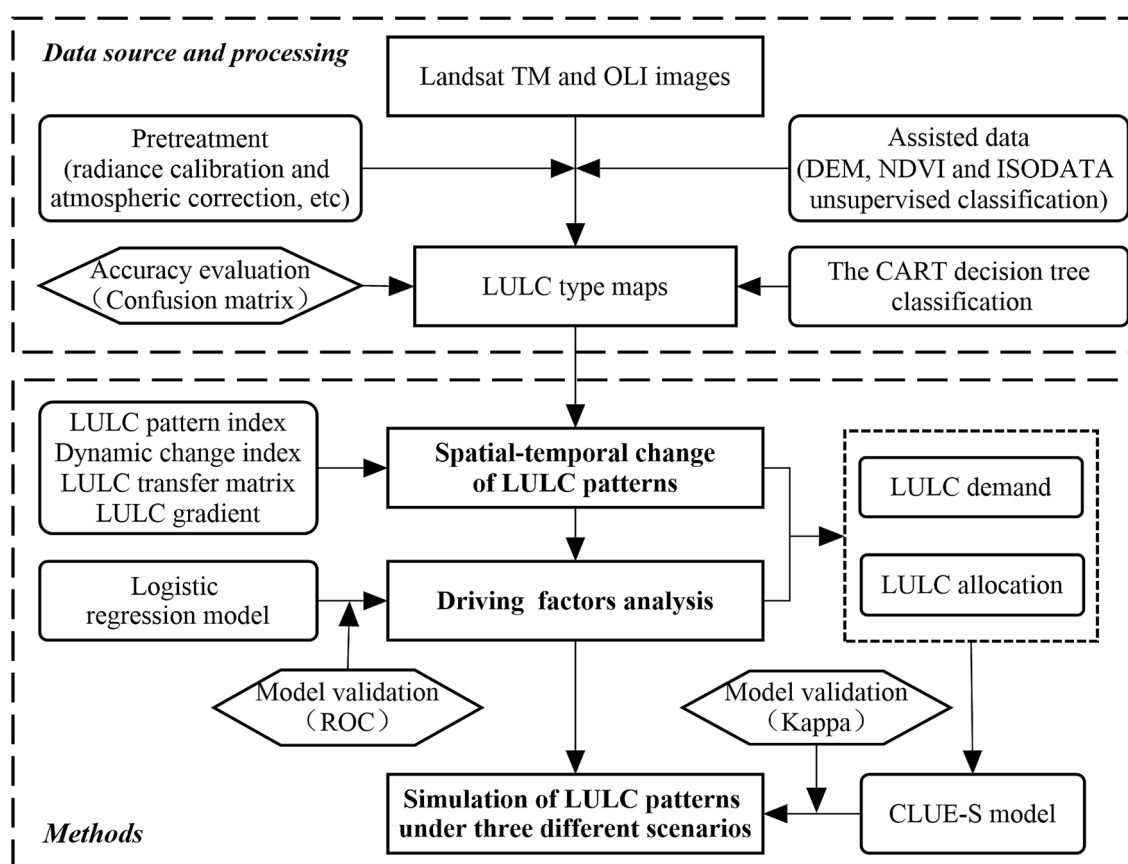


**Fig. 3** Flow chart of methodology

where  $LC$  denotes the comprehensive LULC dynamic degree,  $LU$  denotes the area of the study area, and  $\Delta LU_{i-j}$  denotes the absolute value of the area that was converted from one type to another type.

To further analyse the transfer between different LULC types and identify the number and direction of change during a period (Wan et al. 2015), we calculated the LULC transfer matrix (Solon 2009).

The LULC gradient was used to intuitively reflect the regional differences (Luck and Wu 2002). Based on the mapping scale, the precision of data and research purpose, the grid size was selected as 1 km × 1 km. The equation is as follows:

$$DI = \frac{CA}{\sum_{i=1}^n CA_i} \times 100 \quad (3)$$

where  $DI$  denotes the LULC gradient,  $CA$  denotes the area of a certain LULC type in a grid, and  $CA_i$  denotes the total area of different LULC types in a grid.

### Logistic regression model

Logistic regression is designed to estimate the parameters of a multivariate explanatory model in situations where the dependent variables are binary and the independent variables are continuous or mixed variables (Achmad et al. 2015). The equations are as follows:

$$\ln\left(\frac{p}{1-p}\right) = \alpha + \sum_{i=1}^n \beta_i x_i \quad (4)$$

$$P = \frac{\exp(\alpha + \sum_{i=1}^n \beta_i x_i)}{1 + \exp(\alpha + \sum_{i=1}^n \beta_i x_i)} \quad (5)$$

where  $P$  denotes the occurrence probability of the event,  $x$  denotes the independent variable,  $\alpha$  denotes the constant,

and  $\beta$  denotes the regression coefficient. The goodness-of-fit of the logistic regression model was evaluated by the relative operating characteristic (ROC) (Pontius and Schneider 2001). The model validation results with a ROC value greater than 0.8 suggested good prediction and explanatory power.

### CLUE-S model

The CLUE-S model is composed of non-spatial and spatial modules. The non-spatial module is used to calculate the LULC demands by the Markov model. The spatial module translates these demands into LULC changes at different locations within the study area (Jiang et al. 2015; Verburg et al. 2002). In order to simulate LULC changes as efficient and accurate as possible, multiple resolution scales ranging from 100 to 500 m were used to test the performance of CLUE-S model. Trials found a resolution of 300 m generated better simulation results, with ROC value greater than 0.8, which indicates that the spatial patterns of all LULC types were well explained by the selected driving factors (Pontius 2002). In this study, three potential scenarios were established, namely, natural progression scenario (NS), ecological protection scenario (ES) and cultivated land protection scenario (CS), to simulate the LULC patterns of 2047 (Fig. 4). The principles and targets of designing these scenarios and the parameter settings were as follows.

The NS was formulated based on the historical LULC changes trends. The LULC demand was simulated using the Markov model at a simulation step of 15 years based on the actual percentages of different LULC types in 2017 and the initial transition probability matrix from 2002 to 2017. The ES and CS were policy-based scenarios, and their LULC demand were calculated using the modified Markov transition matrix (Fu et al. 2018; Hu et al. 2013) and linear interpolation method. The ES was established based on the principle of ecological environment protection and the policy orientation. The overall land use planning clearly pointed out that priority should be given

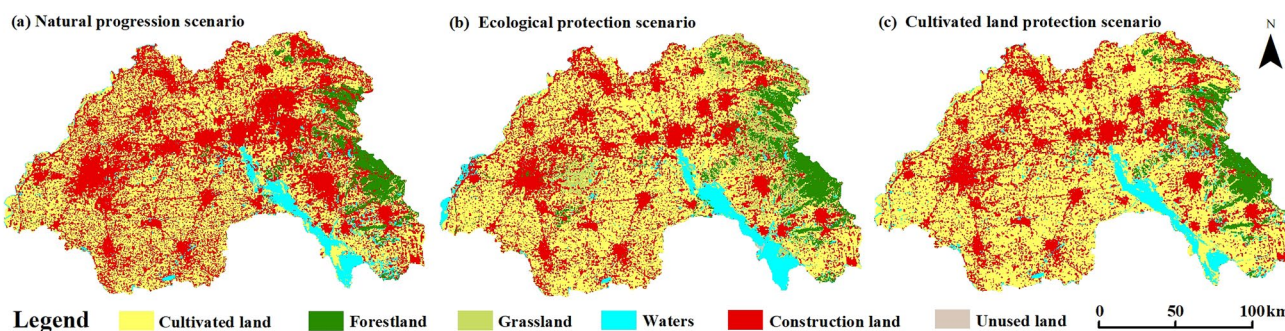


**Fig. 4** LULC simulation maps in 2047 under different scenarios in Shandong Nansihu Lake basin

to the natural ecological protection in the eastern mountains while reforestation and afforestation should be paid more attention. It also emphasized protecting river environment, the Nansihu Nature Reserve and other important ecological nodes. Therefore, after series of trials and modifications, we revised the transition probability matrix to increase the percentage of forestland, grassland and waters. The CS highlighted preservation of cultivated land. The basin had set the objective of strengthening the consolidation of cultivated land. The occupation of cultivated land for construction would be strictly controlled. The overall land use planning recommended exploiting and utilizing the reserved land resources to realize the requisition-compensation balance of cultivated land. This guidance reduced the probabilities of cultivated land converted to construction land, waters and forestland.

The conversion elasticity (ELAS) is related to the reversibility of LULC changes, which reflects the ease or difficulty of LULC conversion (Verburg et al. 2002), ranging from 0 (easy conversion) to 1 (irreversible change). LULC types with high capital investment or irreversible impact on the environment would not easily be converted to other types as long as there was sufficient demand, such as construction land. Some LULC types were more easily converted, for example, cultivated land often provided place for urban sprawl. Finally, the values of ELAS (Table 2) for the defined three scenarios were tuned and implemented so that they were suitable for the model calibration. The kappa coefficient was used to measure the level of agreement between the simulated LULC type map and reality (Cohen 1960; Pontius 2000). The obtained kappa values were all over 75%, which indicates that the two maps showed a relatively high consistency.

**Table 2** The ELAS of different LULC types under different simulated scenarios

LULC types	Natural progression scenario	Ecological protection scenario	Cultivated land protection scenario
Cultivated land	0.5	0.5	0.8
Forestland	0.7	0.9	0.6
Grassland	0.6	0.8	0.6
Waters	0.8	0.8	0.7
Construction land	0.9	0.9	0.9
Unused land	0.3	0.3	0.3

## Results

### Spatial-temporal change of LULC patterns

#### LULC pattern index analysis

At the patch level (Table 3), cultivated land was the main LULC type, with PLAND ranging from 76.08% to 65.68%, and it decreased by 3011.97 km<sup>2</sup> during the last thirty years. The construction land increased from 2922.46 km<sup>2</sup> to 6273.77 km<sup>2</sup>, covering 10.08%, 12.82% and 21.65% of the basin in 1987, 2002 and 2017, respectively. The LPI and COHESION of cultivated land exhibited a decreasing tendency, while construction land showed an increasing tendency. The LSI and PAFRAC of cultivated land showed an increasing trend. The waters first decreased and then increased from 1987 to 2017. The LPI and COHESION of waters first decreased and then increased with an opposite trend as that of grassland. The LSI of waters, construction land, grassland, forestland and unused land showed a decreasing trend in general. The change of forestland was not obvious overall, and it first decreased and then slightly increased, while the grassland and unused land tended to decrease. The COHESION of unused land and forestland decreased and increased, respectively.

On the whole basin, the ED and PAFRAC displayed a continuous growing trend (Table 4). The CONTAG and AI had a tendency to decrease, while the SPLIT had an increasing tendency. The general trends of SHDI and SHEI were increased.

#### LULC dynamic transfer analysis

As seen in Table 5, Fig. 5, from 1987 to 2002, the change range of construction land was the largest, with a dynamic degree of approximately 1.81%. The cultivated land, with the second largest change range, was reduced by 549.37 km<sup>2</sup> with a rate of 0.17%. The conversion from cultivated land to construction land was the main mode, and 8.64% of cultivated land (1905.53 km<sup>2</sup>) was converted into construction land, accounting for 81.27% of the cultivated land change. This transformation mainly occurred in the areas surrounding the original cities. The main contributor to the increase in construction land was cultivated land, occupying 94.04% of the construction land increment. The waters decreased by 112.32 km<sup>2</sup> which were mainly caused by the conversion to cultivated land and unused land. The changes were mostly along the banks of Weishan Lake, Nanyang Lake, Zhaoyang Lake and the Yellow River. Forestland suffered severe degradation in the north-east mountains and 17.66% of forestland was transferred

**Table 3** Patch type LULC pattern indices of Shandong Nansihu Lake basin

LULC types	Year	CA(km <sup>2</sup> )	PLAND (%)	LPI	LSI	PAFRAC	COHESION
Cultivated land	1987	22,048.78	76.08	74.12	97.55	1.255	99.995
	2002	21,499.42	74.18	71.62	118.41	1.263	99.994
	2017	19,036.81	65.68	61.65	133.34	1.265	99.991
Forestland	1987	1913.82	6.60	2.26	67.23	1.244	99.569
	2002	1805.44	6.23	2.25	68.05	1.224	99.580
	2017	1836.67	6.34	2.25	62.32	1.235	99.673
Grassland	1987	739.72	2.55	0.18	74.77	1.268	97.890
	2002	727.38	2.51	0.21	77.62	1.263	98.042
	2017	413.28	1.43	0.10	66.00	1.250	96.729
Waters	1987	834.36	2.88	0.79	56.51	1.273	98.729
	2002	722.04	2.49	0.44	74.92	1.280	98.382
	2017	1361.70	4.70	3.09	55.55	1.240	99.629
Construction land	1987	2922.46	10.08	0.16	212.40	1.192	94.670
	2002	3716.88	12.82	0.23	231.04	1.231	96.123
	2017	6273.77	21.65	1.71	202.66	1.190	98.785
Unused land	1987	523.73	1.81	0.81	23.86	1.230	99.558
	2002	511.71	1.77	0.69	24.92	1.221	99.416
	2017	60.63	0.21	0.03	18.03	1.277	96.870

CA class area; PLAND percentage of LULC; LPI largest patch index; LSI LULC shape index; PAFRAC perimeter-area fractal dimension; COHESION patch cohesion index

**Table 4** LULC pattern indices of Shandong Nansihu Lake basin

Year	ED	PAFRAC	CONTAG	SPLIT	AI	SHDI	SHEI
1987	22.62	1.214	70.70	1.82	96.60	0.89	0.50
2002	26.69	1.222	69.29	1.95	95.99	0.91	0.51
2017	27.82	1.228	66.71	2.62	95.82	1.00	0.56

ED edge density; PAFRAC perimeter-area fractal dimension; CONTAG contagion; SPLIT splitting index; AI aggregation index; SHDI Shannon's diversity index; SHEI Shannon's evenness index

**Table 5** LULC dynamic change in Shandong Nansihu Lake basin

LULC types	1987—2002		2002—2017		1987—2017	
	Area change (km <sup>2</sup> )	Dynamic degree (%)	Area change (km <sup>2</sup> )	Dynamic degree (%)	Area change (km <sup>2</sup> )	Dynamic degree (%)
Cultivated land	−549.37	−0.17	−2462.60	−0.76	−3011.97	−0.46
Forestland	−108.38	−0.38	31.23	0.12	−77.16	−0.13
Grassland	−12.34	−0.11	−314.10	−2.88	−326.44	−1.47
Waters	−112.32	−0.90	639.66	5.91	527.34	2.11
Construction land	794.43	1.81	2556.89	4.59	3351.31	3.82
Unused land	−12.02	−0.15	−451.08	−5.88	−463.09	−2.95
Whole dynamic degree (%)	1.12		1.61		0.86	

to cultivated land. The grassland and unused land were relatively stable LULC types. The LULC dynamic degree of the entire study area was 1.12%.

From 2002 to 2017, the rangeability of cultivated land and construction land increased drastically and was greater

than that in the previous period. The dynamic degree of the cultivated land reached −0.76%, and 3423.40 km<sup>2</sup> of cultivated land was converted into construction land, accounting for 80.71% of the cultivated land change and 94.46% of the construction land change. The waters increased remarkably

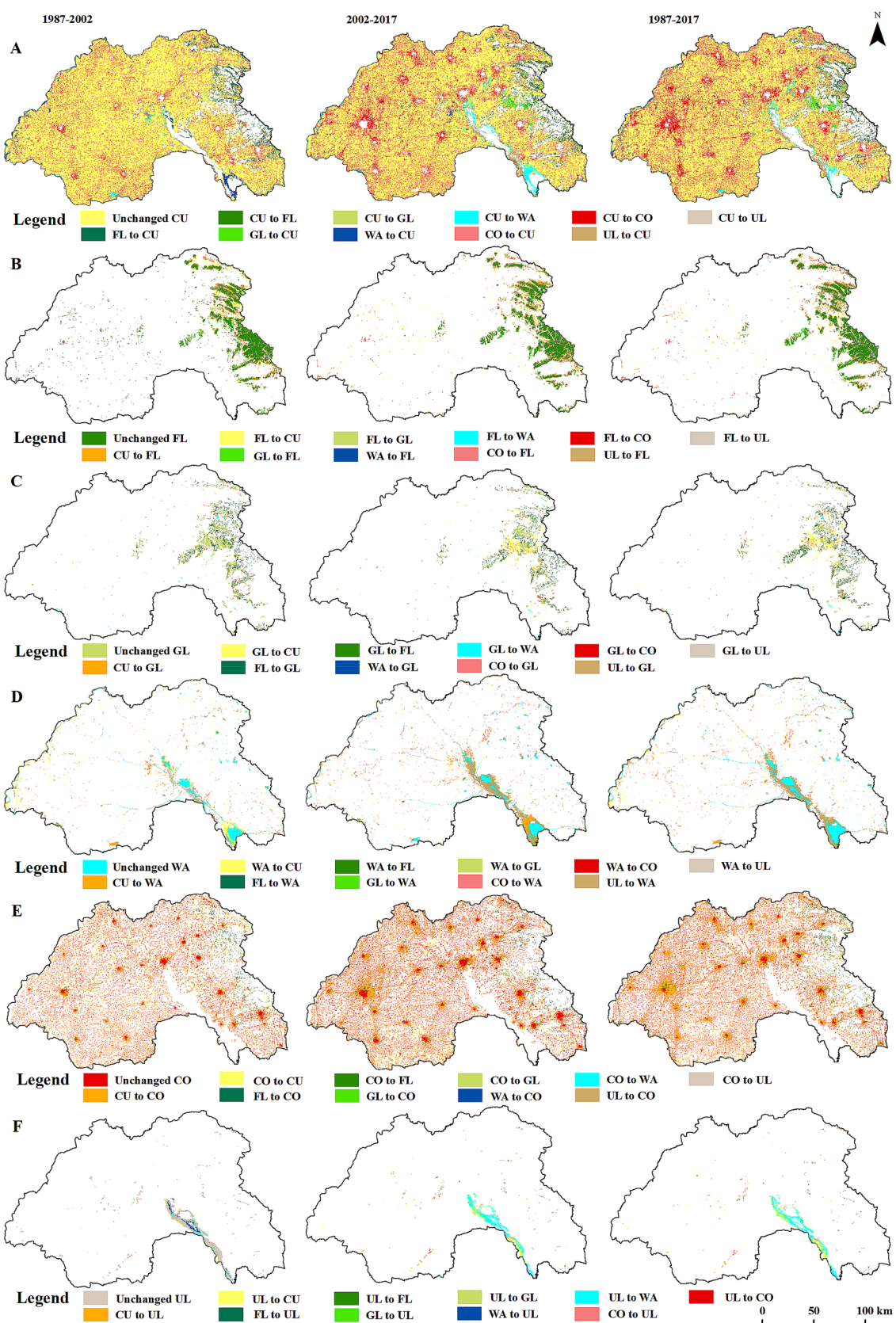


**Fig. 5** Spatial distribution of LULC type transfer in Shandong Nansihu Lake basin. A: Cultivated land (CU); B: Forestland (FL); C: Grassland (GL); D: Waters (WA); E: Construction land (CO); F: Unused land (UL)

with dynamic degrees of 5.91%, especially in the areas surrounding Nansihu Lake. The forestland increased, but the increment was limited. The main sources of waters and forestland were cultivated land, with  $480.39 \text{ km}^2$  and  $314.80 \text{ km}^2$  converted into the two LULC types. The main loss of unused land involved the transition to waters and cultivated land, with a dynamic degree of approximately  $-5.88\%$ . The grassland was still decreasing. The LULC dynamic degree of the entire study area was 1.61%.

## Regional differences analysis

According to the preliminary analysis, the two main LULC types in the basin were cultivated land and construction land, and waters were the most typical LULC in Shandong Nansihu Lake basin. Therefore, this section used cultivated land, construction land and waters as examples and analysed the regional differences in LULC changes on the basis of LULC gradient (Fig. 6) and LULC variable quantity (Fig. 7) in a grid.

In 1987, cultivated land was densely distributed in most of the basin, except for the central areas of cities, the eastern mountains and Nansihu Lake. The cultivated land with a high DI ( $80 < \text{DI} \leq 100$ ) reached  $19,455.61 \text{ km}^2$ , covering 67.13%. The largest distribution area of construction land was the region with DI varying from 10 to 20. The construction land with DI ranging from 50 to 100 accounted for only 0.99%. The waters with a high DI ( $80 < \text{DI} \leq 100$ ) covered  $306.2 \text{ km}^2$ , with a distribution mainly in Nansihu Lake. The waters with DI ranging from 50 to 100 covered  $631.36 \text{ km}^2$  and were distributed along the Yellow River, Si River, Zhuozhaoxin River and Dongyu River.

In 2002, cultivated land showed an overall decreasing trend. The cultivated land with DI ranging from 80 to 100 decreased by  $1915.21 \text{ km}^2$ . The construction land with a high DI ( $80 < \text{DI} \leq 100$ ) gradually emerged in Juancheng, Dongming, Dingtao, Chengwu, Caoxian and other counties. The construction land with DI ranging from 50 to 100 reached  $593.24 \text{ km}^2$ , with the areal proportion increasing to 2.05%. A large amount of cultivated land surrounding cities was occupied, and the decrement in cultivated land

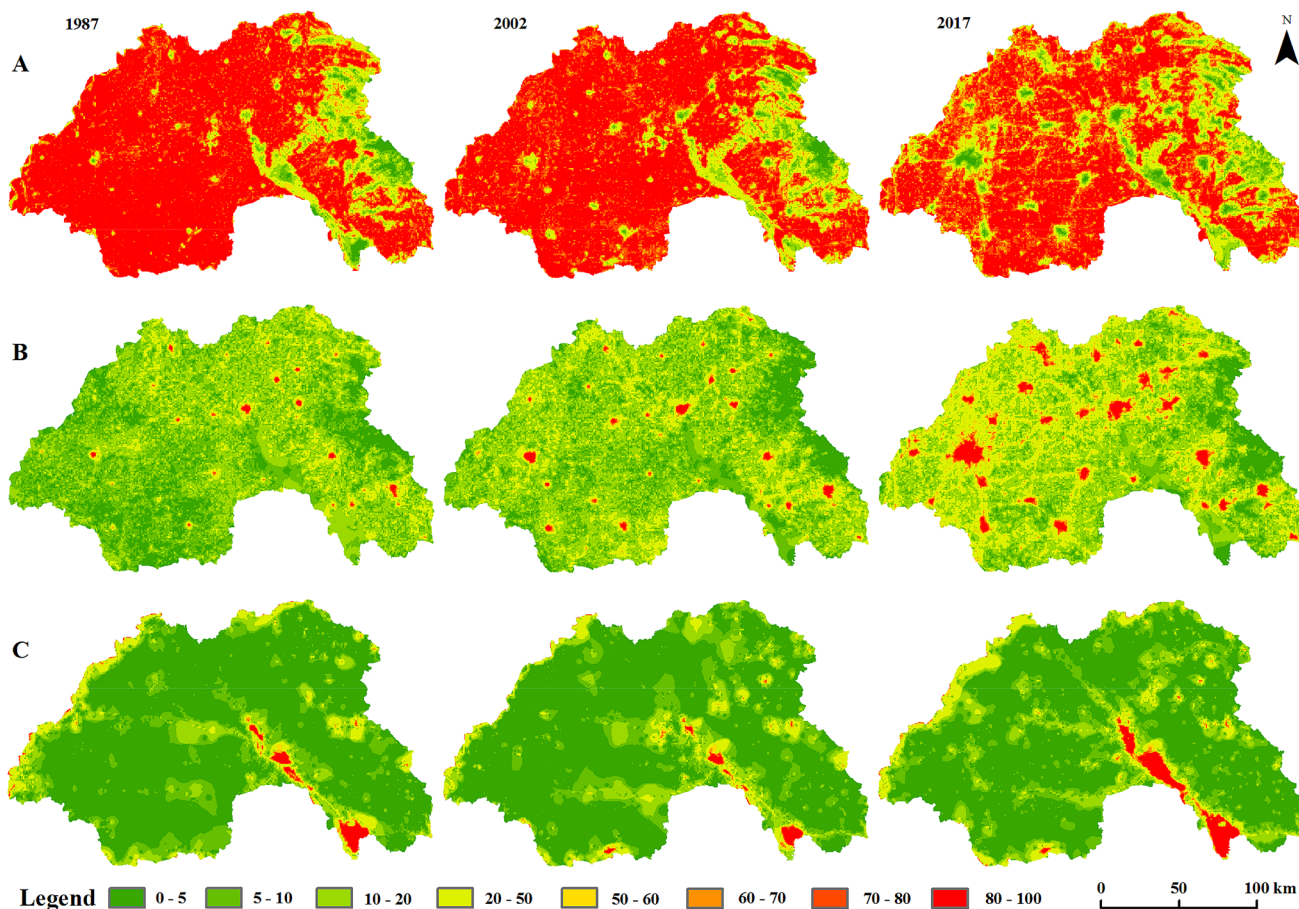


**Fig. 6** Distribution of LULC gradient in Shandong Nansihu Lake basin. A: Cultivated land; B: Construction land; C: Waters. The same is true below

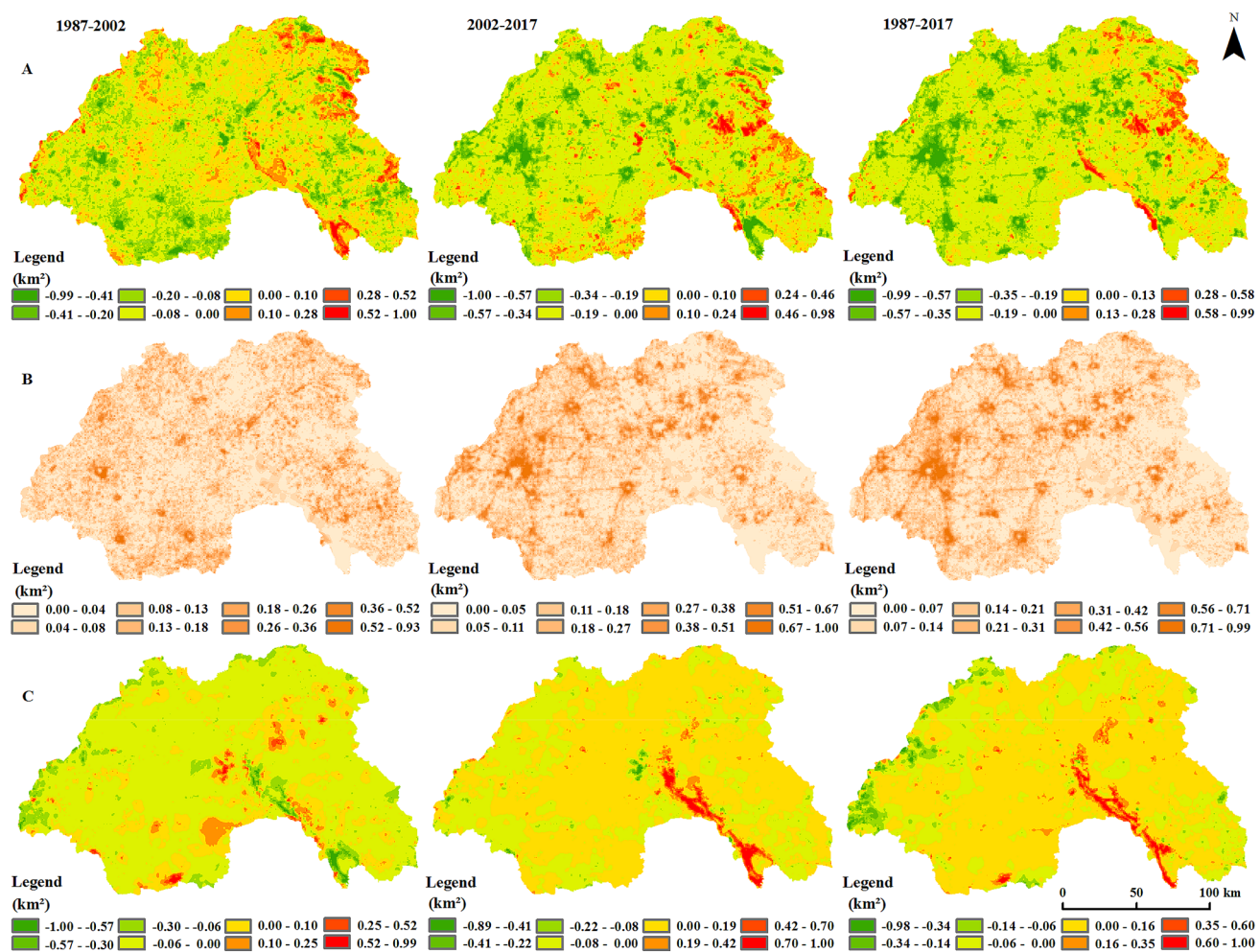


**Fig. 7** Distribution of LULC variable quantity in Shandong Nansihu Lake basin

reached  $0.41 \text{ km}^2$  to  $0.99 \text{ km}^2$  within a grid, while the increment in construction land reached  $0.52 \text{ km}^2$  to  $0.93 \text{ km}^2$ . The waters with a high DI ( $80 < \text{DI} \leq 100$ ) decreased remarkably to  $180.2 \text{ km}^2$ , especially along the bank of Nansihu Lake, with a maximum decrement in a grid of  $1 \text{ km}^2$ .

In 2017, construction land increased significantly, while cultivated land tended to decline. The cultivated land with a high DI ( $80 < \text{DI} \leq 100$ ) decreased by  $8166.05 \text{ km}^2$ , and the areal proportion decreased from 67.13% to 38.96%. The construction land with DI ranging from 50 to 100 increased from  $287.24 \text{ km}^2$  to  $2494.91 \text{ km}^2$ , and the areal proportion increased to 8.61%. The change was more prominent in Mudan District of Heze, downtown Jining and Tengzhou City, where the decrement in cultivated land reached  $0.57 \text{ km}^2$  to  $1 \text{ km}^2$  within a grid and the increment in construction land reached  $0.67$ – $1 \text{ km}^2$ . The waters with a high DI ( $80 < \text{DI} \leq 100$ ) increased significantly, reaching  $688.96 \text{ km}^2$ , with a maximum increment in a grid of  $1 \text{ km}^2$ , especially in Weishan Lake, Liangji Canal and the junction of Qufu, Yanzhou and Zoucheng Cities.

### Driving factors analysis

The Wald statistic represents the relative weight per variable, and it evaluates the contribution of each variable to the event prediction. According to the Wald statistics shown in Table 6, the spatial distribution of cultivated land was greatly influenced by the altitude, distance to coal mine areas and slope. When altitude and slope increased by one unit, the distribution probability of cultivated land decreased by 1.05-fold and 1.45-fold, respectively. GDP was a negative explanatory variable for cultivated land. As the distance to cities, railways and highways increased, the distribution probability of cultivated land increased. Altitude, slope and precipitation were positively correlated with forestland and grassland. The regression coefficients of temperature and distance to rivers were all negative. Additionally, the nearer the cities, railways and highways, the lower was the distribution probability of grassland. Waters had negative relationships with altitude, slope, POP, distance to rivers and coal mine areas. A positive correlation was found between precipitation and

**Table 6** Logistic regression results of the spatial distribution of LULC types

Driving factors	Cultivated land			Forestland			Grassland			Waters			Construction land			Unused land		
	$\beta$	Exp( $\beta$ )	Wald	$\beta$	Exp( $\beta$ )	Wald	$\beta$	Exp( $\beta$ )	Wald	$\beta$	Exp( $\beta$ )	Wald	$\beta$	Exp( $\beta$ )	Wald	$\beta$	Exp( $\beta$ )	Wald
X <sub>1</sub>	-0.05538	0.94612	946.15	0.01018	1.01023	66.24	0.01525	1.01537	129.29	-0.01441	0.98569	6.82	-0.00874	0.99130	50.25	0.03503	1.03565	70.73
X <sub>2</sub>	-0.60326	0.54703	427.93	0.08477	1.08847	25.27	0.13295	1.14219	86.14	-0.20289	0.81637	3.86	-0.22254	0.80049	28.63	-	-	-
X <sub>3</sub>	-0.41594	0.65972	355.03	-0.08340	0.91998	15.53	-0.04393	0.95702	5.86	-	-	-	-	-	-	-0.00156	0.99844	21.54
X <sub>4</sub>	-	-	0.00147	1.00147	147.33	0.00100	1.00100	275.64	0.00075	1.00075	8.89	-	-	-	-	-0.00174	0.99827	28.05
X <sub>5</sub>	-0.00061	0.99939	219.37	-	-	-	-	-	-	-	-	-	0.00019	1.00019	54.75	-	-	-
X <sub>6</sub>	-	-	-	-	-	-	-0.00210	0.99790	53.06	-0.00275	0.99725	65.33	0.00073	1.00073	321.37	-0.00430	0.99571	41.71
X <sub>7</sub>	0.00001	1.00001	4.83	-	-	-	0.00005	1.00005	172.37	-	-	-	-0.00002	0.99998	55.57	-	-	-
X <sub>8</sub>	0.00003	1.00003	316.94	-	-	-	0.00007	0.99993	41.32	-	-	-	-0.00001	0.99999	38.49	0.00002	1.00002	5.79
X <sub>9</sub>	0.00004	1.00004	139.76	-	-	-	0.00006	1.00006	99.34	0.00004	1.00004	8.45	-0.00003	0.99997	33.34	0.00011	1.00011	57.22
X <sub>10</sub>	-	-	-0.00005	0.99995	4.07	-	-	-	-	-	-	-0.00006	0.99994	14.66	-	-	-	
X <sub>11</sub>	-	-	-0.00009	0.99991	37.22	-0.00003	0.99997	20.26	-0.00007	0.99993	7.44	-	-	-	-	-	-	
X <sub>12</sub>	0.00004	1.00004	686.49	-	-	-	-	-	-	-0.00003	0.99997	23.15	0.00001	1.00001	34.47	-0.00013	0.99987	57.11

-: The variables were not statistically significant. X<sub>1</sub>: Altitude; X<sub>2</sub>: Slope; X<sub>3</sub>: Temperature; X<sub>4</sub>: Precipitation; X<sub>5</sub>: GDP; X<sub>6</sub>: POP; X<sub>7</sub>: Distance to cities; X<sub>8</sub>: Distance to railways; X<sub>9</sub>: Distance to county roads; X<sub>10</sub>: Distance to rivers; X<sub>11</sub>: Distance to coal mine areas to highways; X<sub>12</sub>: Distance to mountains.

waters, suggesting that a relatively more rainfall area would experience a bigger distribution probability of waters. The important explanatory variables for construction land distribution were POP, distance to cities, GDP and altitude. When altitude and slope increased by one unit, the distribution probability of construction land decreased by 1.01-fold and 1.20-fold, respectively. Socio-economic factors were positive determinants of construction land. The closer to cities, railways, highways and county roads, the distribution probability of construction land was bigger. In addition, there was also a positive association between construction land and distance to coal mine areas. Altitude, distance to railways and highways were positive explanatory variables for unused land. Precipitation, GDP, POP and distance to coal mine areas had negative relationships with unused land.

### Simulation of LULC patterns under different scenarios

The simulations exhibited similar change trends of cultivated land and construction land under different scenarios, i.e., the expansion of construction land generally would mainly occur at the edges of original cities and at the expense of cultivated land. However, there would be marked differences in the magnitude and position of areal change. Under the NS, the change in construction land would be the largest. The conversion would occur mainly in Mudan District, Dingtao and Juye Counties of Heze, Jiaxiang County, Rencheng District, Yanzhou, Qufu and Zoucheng Cities of Jining, Tengzhou City of Zaozhuang and other regions with greater development potential along the main railways and highways. Under the ES, the increase range of construction land would decrease. The most significant change would be observed in Mudan District, downtown Jining and Rencheng District. Under the CS, the rangeability of cultivated land and construction land would decrease drastically. This result revealed that the cultivated land would receive effective protection.

Under the NS and CS, the forestland and grassland would decrease in the eastern mountains, the reduction under the CS would be more variable. The waters would have an increasing tendency, the increment under the CS would be slightly lower. Under the ES, these ecological lands would have an ascending tendency. Among them, the grassland would have the largest increase mainly at the expense of cultivated land, which would sharply increase by 1247.61 km<sup>2</sup>, especially in Juye County, Zoucheng City, Sishui and Ningyang Counties. The forestland would increase mainly in the eastern mountains, such as southern Sishui County, eastern Zoucheng City and Shanting District. Compared to the other two scenarios, the increase range of waters would be the largest under the ES, reaching 291.96 km<sup>2</sup>, focused primarily in Weishan County and western Dongming County. Under

the three different scenarios, the change trend of unused land would be basically the same. There would be a decreasing trend mainly on the bank of Nansihu Lake and in the eastern mountains for the tendency of unused land.

## Discussion

### Spatial-temporal dynamic change of LULC patterns

Our results revealed that construction land increased sharply and cultivated land decreased dramatically from 1987 to 2017 in Nansihu Lake basin, waters fluctuated with climate and anthropogenic factors. As a result, cultivated land and construction land were the dominant LULC types. Urbanization and the reclaiming of cultivated land increased fragmentation, heterogeneity and shape complexity of LULC patterns. The rivers and lakes were invaded and replaced by grassland on the river bank and lakeshore due to the severe drought in 2002. Because of the increasing of agricultural irrigation and imperfect urban planning systems, waters decreased from 1987 to 2002. With the promulgation of the water laws of the People's Republic of China in 2002, the occurrence of an abrupt drought-flood transition during the flood season of 2003, the establishment of the Nansihu Nature Reserve, the introduction of the overall land use planning in 2006 and the increase in coal mining subsidence areas, waters showed an increasing tendency between 2002 and 2017.

A novelty of this study is that it reflects the regional differences based on gradient analysis. Our results demonstrated that during 1987–2017, the main change direction involved in cultivated land reduction was the conversion to construction land, and  $4109.22 \text{ km}^2$  was converted into construction land, accounting for 86.38% of the cultivated land change; finally, the contribution rate to the construction land was 95.24%. Due to the forms of urban growth, the construction land expanded outward from the original city centre and along the main lines of communication. The largest transformation to construction land occurred in the areas surrounding cities and towns, especially in Mudan District of Heze, downtown Jining and downtown Zaozhuang. These change trends were similar to the findings of Weng (2007), which were strongly influenced by the urban space development strategies of "centre breakthrough, circle development, axis radiation". The waters with high DI ( $80 < \text{DI} \leq 100$ ) increased significantly, which mainly resulted from conversions of cultivated land and unused land. The change was mainly centralized on the bank of Nansihu Lake, the Yellow River, Si River, Zhuzhaixin River, Dongyu River and Beijing-Hangzhou Great Canal and mainly distributed at the junction of Qufu, Yanzhou and Zoucheng Cities, which were consistent with the development orientation of strengthening

land ecological construction in the overall land use planning. In the planning, the southern lakeside depression was determined as key ecological construction areas and the water conservation axis was planned and established relying on the Yellow River.

### Driving factors of LULC changes

Generally, LULC changes in Nansihu Lake basin were strongly influenced by natural environment and socio-economic factors. Altitude and slope were negative explanatory variables for cultivated land, construction land and waters, suggesting that the areas with higher altitude and steeper slope were not suitable for the requirements of agricultural production and livelihood. However, the higher distribution probability of forestland and grassland were found at higher altitude and steeper slope. Temperature and precipitation as climatic factors had important impacts on vegetation and waters. A negative correlation was found between temperature and cultivated land, which is consistent with the study of Hu et al. (2020). There were more forestland, grassland and waters in areas with a relatively more precipitation.

GDP, POP and distance to cities were the most important explanatory variables for the construction land distribution. GDP and POP to some extent reflected the regional economic and social development. With the acceleration of urbanization, the urban land demand for infrastructure driving by population growth and economic development increased gradually. The scale of construction land expanded rapidly, which led to a serious loss of cultivated land and a significant LULC change in the peripheral areas of cities. Influenced by the radiating and driving effects of the city centre, with the decrease in the distance to cities, the distribution probability of construction land was increased. The areas surrounding the main roads had become active economic growth areas because of the convenient traffic conditions; moreover, the increase in distribution probability of residential area, township and other construction land led to a remarkable LULC change. Similar studies found that areas with good transport access experience a higher probability of LULC changes (Ningal et al. 2008; Verburg et al. 2004).

Coal mining induced surface subsidence and waterlogging in the late 1980s and continue today. The surrounding areas of the coal mines were not suitable for production and livelihood. In addition, policy planning had been considered the important driving factor for LULC changes (Sun et al. 2016; Wu et al. 2018). The promulgation of the water laws of the People's Republic of China in 2002 and the establishment of the Nansihu Nature Reserve in 2003 had made waters increase. LULC changes were deeply influenced by the introduction of the overall land use planning in 2006,

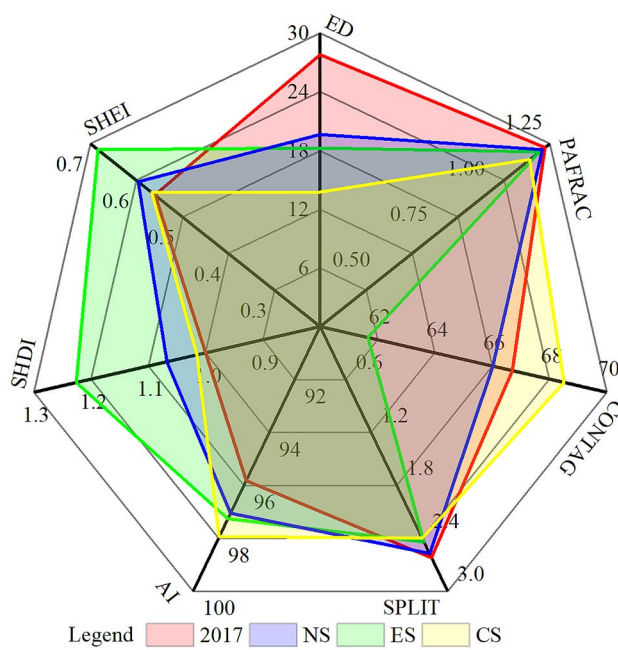


**Fig. 8** The comparison of LULC pattern indices between 2017 and 2047 under different scenarios

which emphasized that the total area of construction land should be strictly controlled in the basin and high-quality agricultural land should be strictly protected.

### LULC change prediction

The Overall Land Use Planning of Jining, Zaozhuang, Heze and Tai'an Cities emphasize the clusterization of cities, land consolidation and ecological space protection. Compared with the historical LULC patterns and the future development orientation and strategies outlined in the planning, the LULC patterns would become more regular, simpler and more aggregated in 2047, evidenced by the reduction in ED, PAFRAC and SPLIT, and the increase in AI (Fig. 8). Especially under the CS, the CONTAG index would increase significantly, the aggregation and connectivity would be the highest. It indicated that appropriate human interventions could optimize and regular the spatial structure of LULC effectively to avoid excessive dispersion. The SHDI and SHEI showing an increasing trend, which suggested that the distribution of different LULC types would be relatively uniform and balanced.

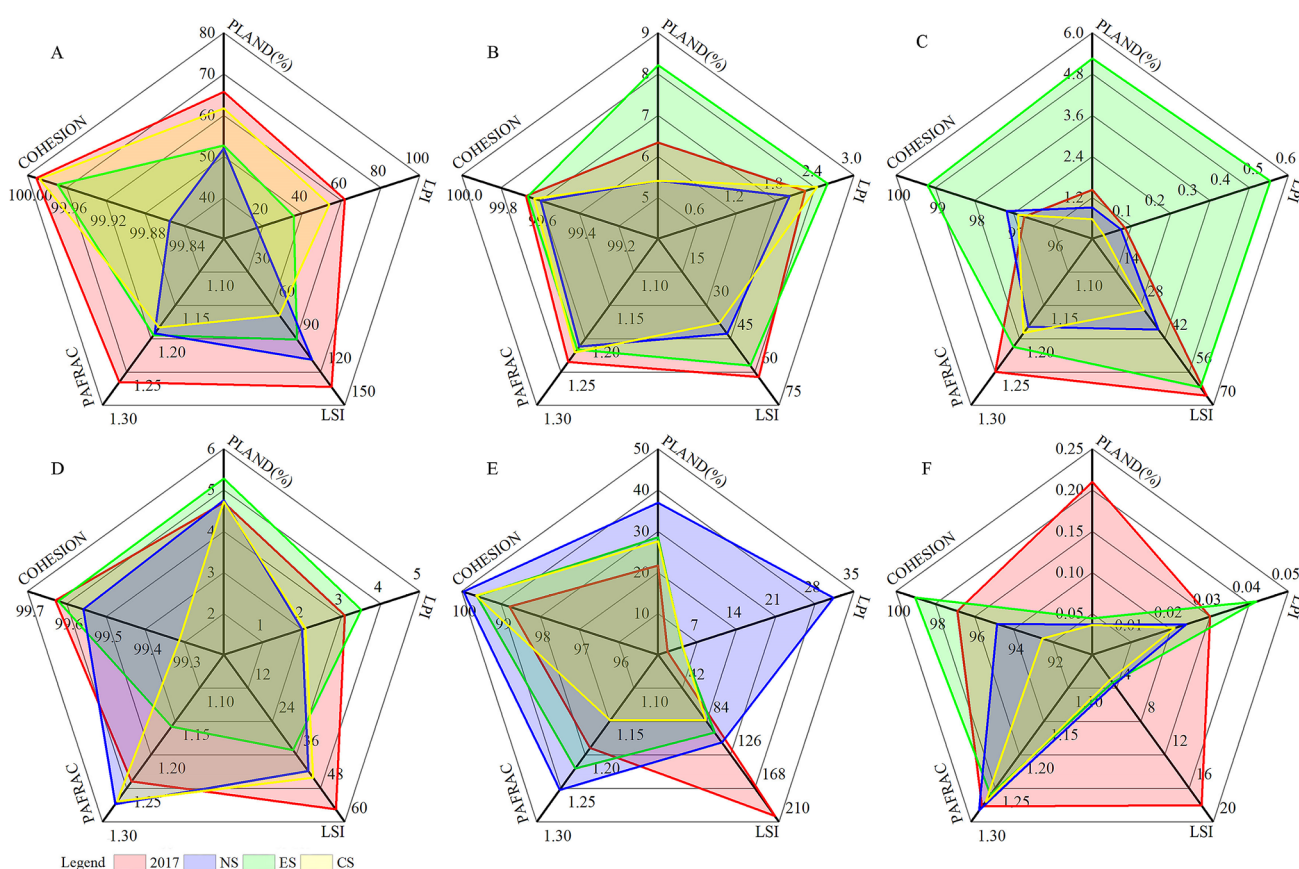


**Fig. 9** The patch type LULC pattern indices in 2017 and 2047 under different scenarios. A: Cultivated land; B: Forestland; C: Grassland; D: Waters; E: Construction land; F: Unused land

As the LULC pattern indices at patch level suggested (Fig. 9), the PLAND, LPI, LSI, PAFRAC and COHESION of cultivated land would have a decrease tendency. It indicated that the cultivated land would be segmented into small patches with more regular shapes, the spatial distribution would become more dispersed in 2047 than in 2017. Under the NS, the LSI of cultivated land would be at the highest values, meanwhile the LPI and COHESION would be at the lowest values, suggesting the relatively higher shape complexity, fragmentation and the relatively lower connectivity. While the cultivated land would show a contrary tendency under the CS affected by the land consolidation planning. The overall land use planning indicated that the urbanization and industrialization in the basin are and will be still in the rapid stage of development. The expansion of construction land and occupation of cultivated land will continue to be the main characteristics of LULC changes in the future. Under the three different scenarios, the construction land would be characterized by the increasing values of PLAND, LPI and COHESION, indicating that construction land would be composed of larger patches with higher connectivity and agglomeration. Furthermore, a reduction in LSI suggested that construction land structure would present simpler and more regular. These changes would be most pronounced under the NS. The forestland and waters would have a trend of dispersed distribution with regular patches. Under the ES, owing to the policy of Green for Grain Project and the priority protection of natural ecological land, forestland, grassland and waters would be larger than other scenarios in 2047, and the connectivity and aggregation would be relatively higher. The unused land would decrease dramatically and become more regular.

## Conclusions

This study demonstrated the effectiveness of the combined method of LULC pattern index, dynamic change index, LULC transfer matrix and gradient analysis for deciphering the dynamic change of LULC patterns in response to natural environmental and anthropogenic activities. Based on logistic regression model and CLUE-S model, the driving factors analysis and scenario simulation analysis were conducted. The results showed that the basin was dominated by cultivated land and construction land. The areas surrounding counties, cities, districts and main roads became hotspots of LULC changes, which led a large amount of cultivated land to be occupied by construction land. LULC changes were driven by the complex interactions of natural environment and socio-economic factors. Under different scenarios, the expansion of construction land and occupation of cultivated land will continue to be the main characteristics of LULC changes in the future. The LULC patterns will become more

regular and more aggregated and the distribution will show a uniform trend. Overall, this study can help identify the characteristics of historical LULC changes and near-future critical locations in the face of the continuous pressure on environment. The results can assist decision-makers in implementing effective protection strategies and sustainable land-use management.

This paper analysed the dynamic change of LULC patterns from the perspective of the grid method, which can compensate for the shortage of expressing the LULC distribution of the study area by using the average value. However, the results will vary with patch sizes. In the future, the scale effect should be fully explored through transforming the grid size in the spatial dimension. Additionally, the accuracy and comprehensiveness of the driving factors should be improved. Determining how to integrate policy implementation, values and other dynamic driving factors quantitatively and spatially to construct the driving forces model of LULC changes should be the focus of further research.

**Acknowledgements** This work was supported by the Foundation of State Key Laboratory of Coal Mine Disaster Dynamics and Control, Chongqing University (2011DA105287-ZD201402).

## References

- Abdolalizadeh Z, Ebrahimi A, Mostafazadeh R (2019) Landscape pattern change in Marakan protected area. *Iran Reg Environ Chang* 19:1683–1699
- Achmad A, Hasyim S, Dahlan B, Aulia DN (2015) Modeling of urban growth in tsunami-prone city using logistic regression: Analysis of Banda Aceh, Indonesia. *Appl Geogra* 62:237–246
- Alhamad MN, Alrababah MA, Feagin RA, Gharaibeh A (2011) Mediterranean drylands: the effect of grain size and domain of scale on landscape metrics. *Ecol Indic* 11:611–621
- Batunacun NC, Hu Y, Lakes T (2018) Land-use change and land degradation on the Mongolian Plateau from 1975 to 2015—a case study from Xilingol, China. *Land Degrad Dev* 29:1595–1606
- Bertolo LS, Lima GTNP, Santos RF (2012) Identifying change trajectories and evolutive phases on coastal landscapes. Case study: São Sebastião Island. *Brazil Landscape Urban Plann* 106:115–123
- Cohen J (1960) A coefficient of agreement for nominal scales. *Educa Psychol Measure* 20:37–46
- Cui X, Wang X (2015) Urban land use change and its effect on social metabolism: an empirical study in Shanghai. *Habitat Int* 49:251–259
- De Clercq EM, Vandemoortele F, De Wulf RR (2006) A method for the selection of relevant pattern indices for monitoring of spatial forest cover pattern at a regional scale. *Int J Appl Earth Obs Geoinf* 8:113–125
- Duarte GT, Santos PM, Cornelissen TG, Ribeiro MC, Paglia AP (2018) The effects of landscape patterns on ecosystem services: meta-analyses of landscape services. *Landscape Ecol* 33:1247–1257
- Feng Y, Liu Y, Tong X (2018) Spatiotemporal variation of landscape patterns and their spatial determinants in Shanghai, China. *Ecol Indic* 87:22–32
- Fu Q, Hou Y, Wang B, Bi X, Li B, Zhang X (2018) Scenario analysis of ecosystem service changes and interactions in a

- mountain-oasis-desert system: a case study in Altay Prefecture. *China Sci Rep* 8:12939
- Hou L, Wu F, Xie X (2020) The spatial characteristics and relationships between landscape pattern and ecosystem service value along an urban-rural gradient in Xi'an city. *China Ecol Indic* 108:105720. <https://doi.org/10.1016/j.ecolind.2019.105720>
- Hu T, Liu J, Zheng G, Zhang D, Huang K (2020) Evaluation of historical and future wetland degradation using remote sensing imagery and land use modeling. *Land Degrad Dev* 31:65–80
- Hu Y, Zheng Y, Zheng X (2013) Simulation of land-use scenarios for Beijing using CLUE-S and Markov composite models. *Chin Geogra Sci* 23:92–100
- Jenerette GD, Wu J (2001) Analysis and simulation of land-use change in the central Arizona – Phoenix region, USA. *Landscape Ecol* 16:611–626
- Jiang W, Chen Z, Lei X, Jia K, Wu Y (2015) Simulating urban land use change by incorporating an autologistic regression model into a CLUE-S model. *J Geogra Sci* 25:836–850
- Joorabian Shooshtari S, Silva T, Raheli Namin B, Shayesteh K (2020) Land use and cover change assessment and dynamic spatial modeling in the Ghara-su Basin, Northeastern Iran. *J Indian Soc Remote 48:81–95*
- Li H, Peng J, Liu Y, Hu Y (2017) Urbanization impact on landscape patterns in Beijing City, China: a spatial heterogeneity perspective. *Ecol Indic* 82:50–60
- Li S, Zhang Z, Sun Y (2013) Simulation of non-point source pollution of nitrogen and phosphorus in lake Nansi watershed using SWAT model. *J Lake Sci* 25:236–242
- Liu C, Xu Y, Sun P, Huang A, Zheng W (2017) Land use change and its driving forces toward mutual conversion in Zhangjiakou City, a farming-pastoral ecotone in Northern China. *Environ Monit Assess* 189:505–204
- Luck M, Wu J (2002) A gradient analysis of urban landscape pattern: a case study from the Phoenix metropolitan region, Arizona, USA. *Landscape Ecol* 17:327–339
- Malandra F, Vitali A, Urbinati C, Weisberg PJ, Garbarino M (2019) Patterns and drivers of forest landscape change in the Apennines range, Italy. *Reg Environ Chang* 19:1973–1985
- Mehrrian MR, Hernandez RP, Yavari AR, Faryadi S, Salehi E (2016) Investigating the causality of changes in the landscape pattern of Lake Urmia basin, Iran using remote sensing and time series analysis. *Environ Monit Assess* 188:462–474
- Mengistie K, Thomas S, Demel T, Thomas K (2015) Drivers of land use/land cover changes in Munessa-Shashemene landscape of the south-central highlands of Ethiopia. *Environ Monit Assess* 187:452–468
- Minta M, Kibret K, Thorne P, Nigussie T, Nigatu L (2018) Land use and land cover dynamics in Dendi-Jeldu hilly-mountainous areas in the central Ethiopian highlands. *Geoderma* 314:27–36
- Ningal T, Hartemink AE, Bregt AK (2008) Land use change and population growth in the Morobe Province of Papua New Guinea between 1975 and 2000. *J Environ Manage* 87:117–124
- Olena D, Gunter M, Christopher C, Elena K, Miriam M, Asia K (2013) Spatio-temporal analyses of cropland degradation in the irrigated lowlands of Uzbekistan using remote-sensing and logistic regression modeling. *Environ Monit Assess* 185:4775–4790
- Overmars KP, Verburg PH, Veldkamp T (2007) Comparison of a deductive and an inductive approach to specify land suitability in a spatially explicit land use model. *Land Use Policy* 24:584–599
- Peng J, Zhao M, Guo X, Pan Y, Liu Y (2017) Spatial-temporal dynamics and associated driving forces of urban ecological land: a case study in Shenzhen City, China. *Habitat Int* 60:81–90
- Plexida SG, Sfougaris AI, Ispikoudis IP, Papanastasis VP (2014) Selecting landscape metrics as indicators of spatial heterogeneity—a comparison among Greek landscapes. *Int J Appl Earth Obs Geoinf* 26:26–35
- Pontius RG (2000) Quantification error versus location error in comparison of categorical maps. *Photogramm Eng Remote Sens* 66:1011–1016
- Pontius RG (2002) Statistical methods to partition effects of quantity and location during comparison of categorical maps at multiple resolutions. *Photogramm Eng Remote Sens* 68:1041–1049
- Pontius RG, Schneider LC (2001) Land-cover change model validation by an ROC method for the Ipswich watershed, Massachusetts, USA. *Agric Ecosyst Environ* 85:239–248
- Schneider LC, Pontius RG (2001) Modeling land-use change in the Ipswich watershed, Massachusetts, USA. *Agric Ecosyst Environ* 85:83–94
- Shooshtari SJ, Gholamalifard M (2015) Scenario-based land cover change modeling and its implications for landscape pattern analysis in the Neka Watershed, Iran. *Remote Sens Appl Soci Environ* 1:1–19
- Solon J (2009) Spatial context of urbanization: Landscape pattern and changes between 1950 and 1990 in the Warsaw metropolitan area, Poland. *Landscape Urban Plann* 93:250–261
- Statuto D, Cillis G, Picuno P (2019) GIS-based analysis of temporal evolution of rural landscape: a case study in Southern Italy. *Nat Resour Res* 28:61–75
- Sun J, Yuan X, Liu H, Liu G, Zhang G (2019) Emergy evaluation of a swamp dike-pond complex: a new ecological restoration mode of coal-mining subsidence areas in China. *Ecol Indic* 107:105660. <https://doi.org/10.1016/j.ecolind.2019.105660>
- Sun P, Xu Y, Yu Z, Liu Q, Xie B, Liu J (2016) Scenario simulation and landscape pattern dynamic changes of land use in the Poverty Belt around Beijing and Tianjin: a case study of Zhangjiakou city, Hebei Province. *J Geogra Sci* 26:272–296
- Verburg PH, Overmars KP, Witte N (2004) Accessibility and land-use patterns at the forest fringe in the northeastern part of the Philippines. *Geogra J* 170:238–255
- Verburg PH, Soepboer W, Veldkamp A, Limpiada R, Espaldon V, Mastura SSA (2002) Modeling the spatial dynamics of regional land use: the CLUE-S model. *Environ Manage* 30:391–405
- Waiyasusri K, Yumuang S, Chotpantarat S (2016) Monitoring and predicting land use changes in the Huai Thap Salao Watershed area, Uthaithani Province, Thailand, using the CLUE-s model. *Environ Earth Sci* 75:533–548
- Wan L, Zhang Y, Zhang X, Qi S, Na X (2015) Comparison of land use/land cover change and landscape patterns in Honghe national nature reserve and the surrounding Jiansanjiang Region, China. *Ecol Indic* 51:205–214
- Wang F, Xie XP, Chen ZC (2017) Dynamic evolution of landscape spatial pattern in Taihu Lake basin, China. *Chin J Appl Ecol* 28:3720–3730
- Weng Y (2007) Spatiotemporal changes of landscape pattern in response to urbanization. *Landscape Urban Plann* 81:341–353
- Wu J (2004) Effects of changing scale on landscape pattern analysis: scaling relations. *Landscape Ecol* 19:125–138
- Wu L, Liu X, Ma X (2018) Prediction of land-use change and its driving forces in an ecological restoration watershed of the Loess hilly region. *Environ Earth Sci* 77:238–250
- Yu L, Li M, Wang S, Zhao Y (2010) Wetland Landscape change in Dali-aohe River basin and the driving factors analysis. *Procedia Environ Sci* 2:1255–1264
- Zhang F, Zhang J, Wu R, Ma Q, Yang J (2016) Ecosystem health assessment based on DPSIRM framework and health distance model in Nansi Lake, China. *Stoch Environ Res Risk Assess* 30:1235–1247
- Zhang L, Jin G, Wei X, Xie P, Liu G, Liu Y (2019) Multiscale analysis of patch and landscape characteristics of forest fragmentation in Liaoning Province, China. *Reg Environ Chang* 19:1175–1186